Copper Coordination Compounds of Polyimidazole–Thioether Ligands. X-ray Structures and Characterization of {Bis[4-((methylthio)ethyl)imidazol-2-yl]methane}bis(tetrafluoroborato)copper(II), Dichloro{(imidazol-2-yl)[4-((methylthio)ethyl)imidazol-2-yl]methane}copper(II), and {[4-(imidazol-2-ylmethyl)imidazol-2-yl][4-((methylthio)ethyl)imidazol-2-yl]methane}-bis(perchlorato)copper(II)†

K. C. Tran,‡ J. P. Battioni,‡ J. L. Zimmermann,§ C. Bois,∥ G. J. A. A. Koolhaas,⊥ P. Leduc,‡ E. Mulliez,‡ H. Boumchita,‡ J. Reedijk,⊥ and J. C. Chottard*,‡

Université René Descartes, Laboratoire de Chimie et Biochimie Pharmacologiques et Toxicologiques, URA 400 CNRS, 75270 Paris, France, Centre d'Etudes de Saclay, Département de Biologie Cellulaire et Moléculaire, Section de Bioénergétique, URA 1290 CNRS, 91191 Gif sur Yvette, France, Université Pierre et Marie Curie, Laboratoire de Chimie des Métaux de Transition, URA 419 CNRS, 75252 Paris, France, and Leiden Institute of Chemistry, Gorlaeus Laboratories, Leiden University, P.O. Box 9502, 2300 RA Leiden, The Netherlands

Received October 14, 1993®

The synthesis and characterization of copper coordination compounds with the polyimidazole–thioether ligands bis[4-((methylthio)ethyl)imidazol-2-yl]methane (L^1), [4-((methylthio)ethyl)imidazol-2-yl](imidazol-2-yl]methane (L^2), and [4-((methylthio)ethyl)imidazol-2-yl][4-(imidazol-2-ylmethyl)imidazol-2-yl]methane (L^3) are described. The study of these new complexes is aimed at modeling the active site of blue-copper proteins. Single crystals of these complexes were used for structural determinations. $[Cu(L^1)(BF_4)_2]$: monoclinic, space group $P2_1/n$, a = 12.252(4) Å, b = 19.782(3) Å, c = 8.954(3) Å, β = 108.72(1)°, Z = 4, T = 291 K, R = 0.056, R' = 0.062 for 1261 reflections; Cu–N = 2.01(1) and 1.99(1) Å; Cu–S = 2.363(4) and 2.361(4) Å; fluorine atoms occupy the axial positions at the distances of 2.65(1) and 2.565(8) Å to Cu, in a distorted octahedral geometry. $[Cu(L^2)Cl_2]$: monoclinic, space group $P2_1/a$, a = 13.48(1) Å, b = 11.721(9) Å, c = 9.997(7) Å, β = 108.86(5)°, Z = 4, T = 291 K, R = 0.060, R' = 0.068 for 870 reflections; Cu–N = 2.01(1) and 2.00(1) Å, Cu–S = 2.387(5) Å, Cu–Cl = 2.279(4) and 2.660(4) Å, in a distorted square pyramidal geometry. $[Cu(L^3)(ClO_4)_2]$: triclinic, space group $P\bar{1}$, a = 8.679(6) Å, b = 9.866(2) Å, c = 12.445(1) Å, α = 82.46(2)°, β = 85.80(5)°, γ = 88.21(2)°, Z = 2, T = 291 K, R = 0.082, R' = 0.089 for 511 reflections; Cu–S = 2.40(2) Å, Cu–N = 1.90(4), 1.94(4), and 1.98(3) Å; oxygen atoms occupy the axial positions at the distances of 2.90(4) and 2.96(5) Å to Cu, in a distorted octahedral geometry. Cyclic voltammograms of $Cu(L^1)^{2+}$ and $Cu(L^2)^{2+}$ complexes exhibit two waves due to the presence of the mono-ligand and bis-ligand complexes in solution. The $Cu(L^3)^{2+}$ complex shows only one quasi-reversible wave. The compounds were further characterized by electronic, EPR, and ESEEM spectroscopies.

Introduction

Blue-copper proteins play important roles in electron-transfer and oxidase activity in plants, algae, and bacteria. The blue-copper active site is found in a number of proteins containing a single copper center such as plastocyanin, azurin, and stellacyanin.[1-4] It is also found in multicentered copper proteins such as laccase, ascorbic oxidase, and ceruloplasmin.[5,6] A well-characterized blue-copper protein is plastocyanin. Its active site consists of a single copper atom coordinated by two histidine imidazole nitrogens, a cysteine thiolate sulfur, and a methionine thioether sulfur, forming a distorted tetrahedral geometry.[7]

There are intensive modeling studies in many laboratories in order to synthesize chemical analogues of the active site of these blue-copper proteins.[8] The aim of the modeling work is to mimic (i) the strong absorption band in the red region of the visible spectrum ($\lambda \approx 600$ nm, $\epsilon \approx 5000$ M^{-1} cm^{-1}), (ii) the particularly small EPR hyperfine coupling constant from the copper nucleus ($A_\parallel < 70 \times 10^{-4}$ cm^{-1}), and (iii) the relatively high redox potential of 200–700 mV.[9,10] Methods for constructing model compounds include the design of ligands consisting of N and S donor atoms, and several N_xS_y donor ligands have been designed so far.[8,11-13] Imidazole- and thioether-containing ligands are relevant to this study.

In the present work, the ligands bis[4-((methylthio)ethyl)-imidazol-2-yl]methane (L^1), (imidazol-2-yl)[4-((methylthio)-

* To whom correspondence should be addressed.

† Abbreviation list: EPR, electron paramagnetic resonance; ESEEM, electron spin echo envelope modulation; bim, bis(imidazol-2-yl)methane; tim, bis[4-(imidazol-2-ylmethyl)imidazol-2-yl]methane; Him, imidazole; NQI, nuclear quadrupole interaction; DMSO, dimethyl sulfoxide; near-IR–vis, near-infrared–visible; mp, melting point.

‡ Université Rene Descartes.

§ Centre d'Etudes de Saclay.

∥ Université Pierre et Marie Curie.

⊥ Leiden University.

® Abstract published in *Advance ACS Abstracts*, April 15, 1994.

(1) Adman, E. T.; Turley, S.; Bramson, R.; Petratos, K.; Banners, D.; Tsernoglou, D.; Beppu, T.; Watanabe, H. *J. Biol. Chem.* **1989**, *264*, 87–99.
(2) Sykes, A. G. *Struct. Bonding* **1990**, *75*, 175–225.
(3) Field, B. A.; Guss, J. M.; Freeman, H. C. *J. Biol. Chem.* **1991**, *222*, 1053–1065.
(4) Han, J.; Adman, E. T.; Beppu, T.; Codd, R.; Freeman, H. C.; Haq, L.; Loehr, T. M.; Sander-Loehr, J. *Biochemistry* **1991**, *30*, 10904–10913.
(5) Musci, G.; Desideri, A.; Morpurgo, L.; Garnier-Sullerot, A.; Tosi, L. *Biochem. J.* **1983**, *213*, 503–506.
(6) Messerschmidt, A.; Huber, R. *Eur. J. Biochem.* **1990**, *187*, 341–352.
(7) Guss, J. M.; Freeman, H. *J. Mol. Biol.* **1983**, *169*, 521–563.
(8) Bouwman, E.; Driessen, W. L.; Reedijk, J. *Coord. Chem. Rev.* **1990**, *104*, 143–172.
(9) Solomon, E. I.; Hare, J. W.; Dooley, D. M.; Dawson, J. H.; Stephens, P. J.; Gray, H. B. *J. Am. Chem. Soc.* **1980**, *102*, 168–178.
(10) Solomon, E. I.; Penfield, K. W.; Wilcox, D. E. *Struct. Bonding* **1983**, *53*, 1–57.

0020-1669/94/1333-2808$04.50/0

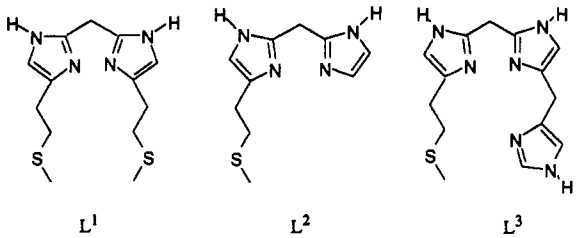

L^1 L^2 L^3

Figure 1. Schematic drawings of ligands bis[4-((methylthio)ethyl)-imidazol-2-yl]methane (L^1), (imidazol-2-yl)[4-((methylthio)ethyl)imidazol-2-yl]methane (L^2), and [4-(imidazol-2-ylmethyl)imidazol-2-yl][4-((methylthio)ethyl)imidazol-2-yl]methane (L^3).

ethyl)imidazol-2-yl]methane (L^2), and [4-(imidazol-2-ylmethyl)-imidazol-2-yl][4-((methylthio)ethyl)imidazol-2-yl]methane (L^3) corresponding to N_2S_2, N_2S, and N_3S donor ligands, respectively, have been used to model the azole and thioether parts of the blue-copper active site. The schematic drawings of these ligands are shown in Figure 1. Coordination compounds of these three ligands with copper(II) and various anions have been synthesized and their physicochemical properties together with their X-ray structures are described. Future work includes the modification of our ligands to introduce a thiolate group in order to better mimic the coordination sphere of the blue-copper protein active site. A detailed comparison of the already synthesized and characterized complexes (without thiolate ligands) with those complexes including thiolate ligands will give important information about the proper features of the thiolate–copper(II) coordination.

Experimental Section

Synthesis of the Ligands. The synthesis of the ligands L^1, L^2, and L^3 from commercially available 5-nitro-4,6-dichloropyrimidine and appropriate α-amino acetals is based on a general method developed by Mulliez.[14]

L^1 has been previously described.[14] L^2 is obtained through a similar set of reactions as those described for L^1. Briefly, the stoichiometric reaction of the acetal of methioninal with the previously described 5-nitro-4-chloro-6-(2′-amino-1,1′-diethoxyethyl)pyrimidine in ethanol containing 1.5 equiv of Et_3N affords a quantitative yield of the mixed pyrimidine. The latter is converted to L^2 by the described procedure:[14] Mp = 168 °C, yield = 45%.

Similarly, L^3 is obtained from the stoichiometric reaction of the acetal of histidinal with crude 5-nitro-4-chloro-6-(2′-amino-2′-(methylthio)-ethyl)-1,1′-diethoxyethyl)pyrimidine. The mixed pyrimidine is then converted to L^3 by the described procedure:[14] Mp = 140 °C, yield = 35%.

All compounds gave satisfactory spectroscopic and analytical data.

Synthesis of the Cu(II) Complexes. The coordination compounds of general formula $[Cu(L)X_2]$ were prepared by dissolving the appropriate metal salt (1 equiv) in methanol and adding this solution to a solution of the ligand L (1 equiv) in methanol. In the case of the bis-ligand compounds, the solution contained at least 2 equiv of the ligand L.

The crystallization of $[Cu(L)X_2]$ by vapor diffusion of diethyl ether into a methanolic solution of the complex gave dark blue crystals for $[Cu(L^1)(BF_4)_2]$ and green crystals for $[Cu(L^2)Cl_2]$. For $[Cu(L^3)(ClO_4)_2]$, purple crystals were obtained by liquid diffusion of diethyl ether into a methoxyethanol solution of the complex. The crystal size of the latter compound was hardly suitable for X-ray diffraction recording, and all attempts to improve it have yet failed.

N.B: *Warning*! One of the compounds described here contains perchlorate anions. Although no accidents have occurred, the use of perchlorate is hazardous because of the possibility of explosion, especially when the compounds are anhydrous.

Table 1. Experimental Data for the Crystallographic Analysis of $Cu(L^1)(BF_4)_2$, $Cu(L^2)Cl_2$, and $Cu(L^3)(ClO_4)_2$

formula	$Cu(L^1)(BF_4)_2$, $C_{13}H_{20}B_2CuF_8N_4S_2$	$Cu(L^2)Cl_2$, $C_{10}H_{14}Cl_2CuN_4S$	$Cu(L^3)(ClO_4)_2$, $C_{14}H_{18}HCl_{12}CuN_6O_8S$
MW	533.6	300.7	564.8
cryst system	monoclinic	monoclinic	triclinic
space group	$P2_1/n$	$P2_1/a$	$P\bar{1}$
a, Å	12.252(4)	13.48(1)	8.679(6)
b, Å	19.782(3)	11.721(9)	9.866(2)
c, Å	8.954(3)	9.997(7)	12.445(1)
α, deg			82.46(2)
β, deg	108.72(1)	108.86(5)	85.80(5)
γ, deg			88.21(2)
V, Å^3	2055(2)	1495(3)	1053(2)
Z	4	4	2
d_{calc}, g cm^{-3}	1.72	1.34	1.78
μ, cm^{-1}	13.4	19.3	18.1
no. of indpt reflcns	3589	2570	1963
no. of reflcns used with $I \geq 3\sigma(I)$	1261	870	511[a]
R[b]	0.056	0.060	0.082
R'[b]	0.062	0.068	0.089

[a] For this complex $I \geq 2\sigma(I)$. [b] $R = [\sum|\Delta F|/\sum F_o]$; $R' = [\sum w(\Delta F^2)/\sum wF_o^2]^{1/2}$.

Elemental analyses of these crystals were performed by the "Service Central d'Analyse" of the CNRS in Vernaison, France. The elemental analyses of the three crystals gave satisfactory results.

Crystallography. The diffraction data for $Cu(L^1)(BF_4)_2$, $Cu(L^2)Cl_2$, and $Cu(L^3)(ClO_4)_2$ were collected at room temperature on a four-circle Philips PW1100 diffractometer. Graphite-monochromatized Mo Kα was used. Unit cell dimensions with estimated standard deviations were obtained from least-squares refinements of the setting angles of 25 well-centered reflections. Two standard reflections were monitored periodically; they showed no change during data collection. Further details on data collection and refinements are given in Table 1 and supplementary Table S1. Corrections were made for Lorentz and polarization effects. Empirical absorption corrections (Difabs)[15] were applied.

Computations were performed by using CRYSTALS[16] adapted on a Micro Vax II. Atomic form factors for neutral Cu, Cl, S, F, O, N, B, C, and H were taken from ref 17. Anomalous dispersion was taken into account. An extinction correction was unnecessary. The three structures were solved by direct methods and subsequent Fourier maps. Hydrogen atoms were theoretically located at C–H distances of 1.03 Å and were given an overall isotropic thermal parameter. For $Cu(L^1)(BF_4)_2$ only Cu, S, and F atoms were anisotropically refined. For $Cu(L^2)Cl_2$ all non-hydrogen atoms were anisotropically refined. For $Cu(L^3)(ClO_4)_2$ all atoms were only isotropically refined, because of the small number of reflections. Refinements were carried out in three blocks, by minimizing the function $\sum w(|F_o| - |F_c|)^2$. The weighting scheme was $w = 1$ for $Cu(L^1)(BF_4)_2$ and $Cu(L^3)(ClO_4)_2$ and $w = w'[1 - (F_o - F_c)/6\sigma(F_o))^2]^2$ with $w' = 1/\sum_{r=1,3} ArTr(X)$ with three coefficients 1.07, 0.75, and 0.75 for the Chebyshev polynomial $Tr(X)$ with $X = F_o/F_o$ maximum for $Cu(L^2)Cl_2$. Criteria for a satisfactory complete analysis were the ratios of root-mean-square shift to standard deviation being less than 0.1 and no significant features in final difference maps.

Lists of the atomic coordinates and U values of the hydrogen atoms and of the non-hydrogen atoms, the interatomic bond lengths and angles, and the non-hydrogen anisotropic thermal parameters are available as supplementary material.

Electrochemical Measurements. Cyclic voltammograms were obtained with the EGG-PAR Model 173 potentiostat and Model 276 interface instruments at room temperature, in methanol solution under Ar. The electrode system consisted of a NaCl saturated calomel electrode as reference electrode, a platinum electrode as auxiliary electrode, and a glassy C electrode as working electrode. $LiClO_4$ was used as supporting electrolyte (0.1 M in CH_3OH). The scan rate was 50 mV s^{-1}. The control for "free $Cu(BF_4)_2$" in solution was done using the cyclic voltammetric study of $Cu(BF_4)_2$ in CH_3OH.

Electronic Spectroscopies. UV–vis spectra were recorded using a Uvikon 810 spectrophotometer, in methanol solution over the wavelength

(11) Kitajima, N.; Fujisawa, K.; Moro-oka, Y. *J. Am. Chem. Soc.* **1990**, *112*, 3210–3212. Kitajima, N.; Fujisawa, K.; Tanaka, M.; Moro-oka, Y. *J. Am. Chem. Soc.* **1992**, *114*, 9232–9233.
(12) Brader, M. L.; Dunn, M. F. *J. Am. Chem. Soc.* **1990**, *112*, 4585–4587. Brader, M. L.; Borchardt, D.; Dunn, M. F. *J. Am. Chem. Soc.* **1992**, *114*, 4480–4486.
(13) Lu, Y.; Gralla, E. B.; Roe, J. A.; Valentine, J. S. *J. Am. Chem. Soc.* **1992**, *114*, 3560–3562. LaCroix, L. B.; Lowery, M. D.; Solomon, E. I.; Bender, C. J.; Peisach, J.; Roe, J. A.; Gralla, E. B.; Valentine, J. S. *J. Am. Chem. Soc.* **1993**, *115*, 5907–5918.
(14) Mulliez, E. *Tetrahedron Lett.* **1989**, *30*, 6169–6172.
(15) Walker, N.; Stuart, D. *Acta Crystallogr.* **1983**, *39*, 158.
(16) Watkin, D. J.; Carruthers, J. R.; Betteridge, P. W. *Crystals, An Advanced Crystallographic Program System*; Chemical Crystallography Laboratory, University of Oxford: Oxford, England, 1988.
(17) *International Tables for X-ray Crystallography*; Kynoch Press: Birmingham, England, 1974; Vol. 4.

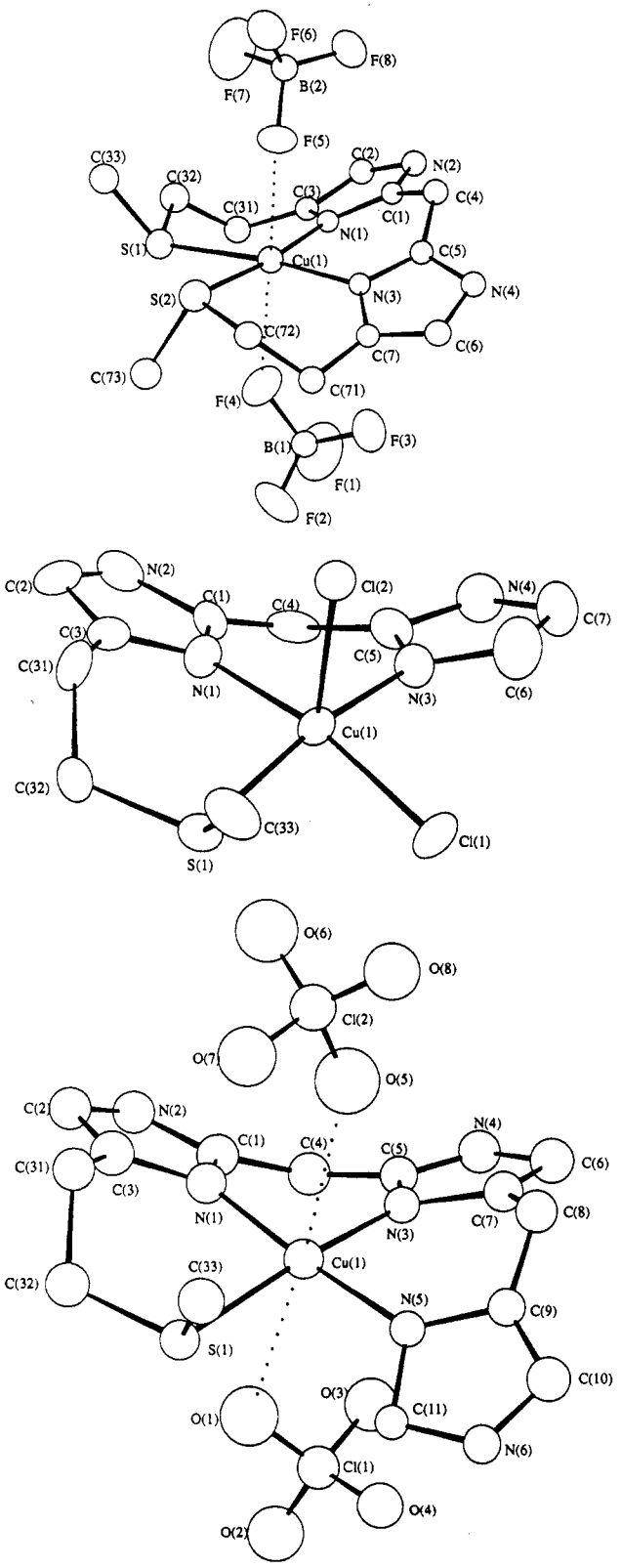

Figure 2. (a) Top: CAMERON projection of $Cu(L^1)(BF_4)_2$ with the atomic labeling. (b) Middle: CAMERON projection of $Cu(L^2)Cl_2$ with the atomic labeling. (c) Bottom: CAMERON projection of $Cu(L^3)(ClO_4)_2$ with the atomic labeling. For clarity the hydrogen atoms are omitted.

range 220–800 nm. Solid-state vis–near-IR spectra were recorded using a Perkin-Elmer 330 spectrometer.

Electron Paramagnetic Resonance (EPR). The complexes were studied in both solid state (polycrystalline powder at 298 and 77 K) and in frozen solution, CH_3OH/DMSO (1/1 v/v), at 77 K using a Jeol RE 2X EPR spectrometer.

Electron Spin Echo Envelope Modulation (ESEEM). The samples were prepared by dissolving each compound in either CH_3OH/H_2O (1/1 v/v) or CH_3OH/DMSO (1/1 v/v) to a final concentration of approximately 2 mM. In some experiments (see below), a solution containing the compound with 2 equiv of ligand was prepared by mixing the compound with an extra 1 equiv of the appropriate ligand.

The ESEEM signals were recorded on a Bruker ER 380 pulsed EPR spectrometer operating with a dielectric resonator. The experiments were performed on frozen solutions at 4.2 K. The signals were obtained by recording the amplitude of the simulated echo arising from a 3 microwave pulse sequence as a function of the time T separating the 2nd and 3rd pulses. The artifacts due to superposition of unwanted 2-pulse echoes to the 3-pulse stimulated echo decay were eliminated by appropriate phase cycling of the first and second pulses.[18] The cosine Fourier transforms of the data were obtained by reconstructing the missing data points due to spectrometer dead time by a method similar to that described by Mims.[19]

Table 2. Selected Interatomic Bond Lengths (Å) and Angles (deg) of $Cu(L^1)(BF_4)_2$, $Cu(L^2)Cl_2$, and $Cu(L^3)(ClO_4)_2$

$Cu(L^1)(BF_4)_2$			
Cu(1)–S(1)	2.363(4)	Cu(1)–S(2)	2.361(4)
Cu(1)–N(1)	2.01(1)	Cu(1)–N(3)	1.99(1)
Cu(1)–F(4)	2.65(1)	Cu(1)–F(5)	2.565(8)
S(2)–Cu(1)–S(1)	82.3(1)	N(1)–Cu(1)–S(1)	93.6(3)
N(1)–Cu(1)–S(2)	173.9(3)	N(3)–Cu(1)–S(1)	173.6(3)
N(3)–Cu(1)–S(2)	93.3(3)	N(3)–Cu(1)–N(1)	91.1(4)
F(4)–Cu(1)–S(1)	81.1(3)	F(4)–Cu(1)–S(2)	92.9(3)
F(4)–Cu(1)–N(1)	90.8(4)	F(4)–Cu(1)–N(3)	94.6(4)
F(5)–Cu(1)–S(1)	99.2(2)	F(5)–Cu(1)–S(2)	84.9(2)
F(5)–Cu(1)–N(1)	91.4(4)	F(5)–Cu(1)–N(3)	85.0(4)
F(5)–Cu(1)–F(4)	177.7(3)		
$Cu(L^2)Cl_2$			
Cu(1)–S(1)	2.387(5)	Cu(1)–Cl(1)	2.279(4)
Cu(1)–N(1)	2.01(1)	Cu(1)–N(3)	2.00(1)
Cu(1)–Cl(2)	2.660(4)		
Cl(1)–Cu(1)–S(1)	84.3(2)	Cl(2)–Cu(1)–S(1)	98.9(1)
Cl(1)–Cu(1)–Cl(2)	98.6(1)	N(1)–Cu(1)–S(1)	91.1(4)
N(1)–Cu(1)–Cl(1)	167.0(4)	N(1)–Cu(1)–Cl(2)	94.1(4)
N(3)–Cu(1)–S(1)	165.5(4)	N(3)–Cu(1)–Cl(2)	95.5(4)
N(3)–Cu(1)–Cl(1)	91.8(4)	N(3)–Cu(1)–N(1)	89.7(6)
$Cu(L^3)(ClO_4)_2$			
Cu(1)–S(1)	2.40(2)	Cu(1)–N(1)	1.94(4)
Cu(1)–N(3)	1.90(4)	Cu(1)–N(5)	1.98(3)
Cu(1)–O(1)	2.90(4)	Cu(1)–O(5)	2.96(5)
N(1)–Cu(1)–S(1)	91.2(13)	N(3)–Cu(1)–S(1)	174.6(12)
N(3)–Cu(1)–N(1)	90.0(17)	N(5)–Cu(1)–S(1)	91.3(12)
N(5)–Cu(1)–N(1)	176.6(19)	N(5)–Cu(1)–N(3)	87.8(15)
O(1)–Cu(1)–S(1)	78.7(9)	O(1)–Cu(1)–N(1)	85.2(14)
O(1)–Cu(1)–N(3)	96.2(14)	O(1)–Cu(1)–N(5)	97.6(13)
O(5)–Cu(1)–S(1)	103.5(10)	O(5)–Cu(1)–N(1)	88.3(14)
O(5)–Cu(1)–N(3)	81.8(15)	O(5)–Cu(1)–N(5)	88.9(14)
O(5)–Cu(1)–O(1)	173.2(13)		

Results

Description of the Structures: $Cu(L^1)(BF_4)_2$. The CAMERON[20] projection with atomic labeling is given in Figure 2a. The copper(II) ion is octahedrally coordinated by two imidazole nitrogens (1.99–2.01 Å) and two thioether sulfurs (2.36 Å) in the equatorial plane. The two BF_4^- anions are found in the apical positions at semicoordinating distances (2.56–2.65 Å). Selected interatomic bond lengths and angles are given in Table 2.

$Cu(L^2)Cl_2$. The CAMERON[20] projection is shown in Figure 2b. The Cu(II) ion is square-pyramidally coordinated by two imidazole nitrogens, a thioether sulfur and a chloride in an equatorial plane. The second anion Cl^- coordinates with Cu(II) in the apical position. Selected interatomic bond lengths and angles are given in Table 2. The Cu–Cl bond distance in the apical position (2.66 Å) is about 0.4 Å longer than the equatorial

(18) Fauth, J. M.; Schweiger, A.; Braunschweiger, L.; Forrer, J.; Ernst, R. R. *J. Magn. Reson.* **1986**, *66*, 74–85.
(19) Mims, W. B. *J. Magn. Reson.* **1984**, *59*, 291–306.
(20) Pearce, L. J.; Walkin, D. J. *CAMERON*; Crystallography Laboratory: Oxford, England.

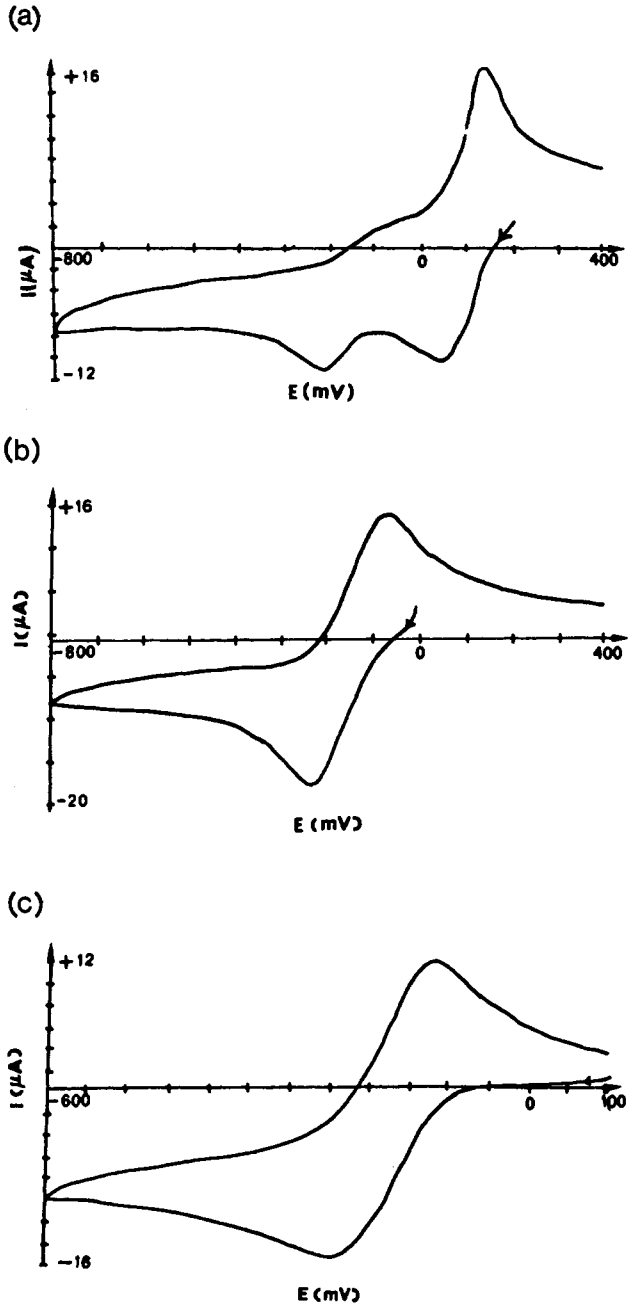

Figure 3. Cyclic voltammograms recorded at a glassy C electrode in a deaerated CH_3OH solution containing (a) L^1 (6.67×10^{-3} mol L^{-1}) and $Cu(BF_4)_2$ (6.67×10^{-3} mol L^{-1}), (b) L^1 (13.3×10^{-3} mol L^{-1}) and $Cu(BF_4)_2$ (6.67×10^{-3} mol L^{-1}) and (c) L^3 (6.67×10^{-3} mol L^{-1}) and $Cu(BF_4)_2$ (6.67×10^{-3} mol L^{-1}). The scan rate is 0.05 V s^{-1}. The temperature is 293 K. Potentials are referred to SCE.

Cu–Cl bond distance (2.28 Å). Moreover, at a quite remote distance (3.54 Å), the thioether sulfur of one complex provides a weak interaction with the copper(II) of another complex at the second apical position (see supplementary material). These interactions force the CH_3 group into the cis position relative to the axial Cl^-.

$Cu(L^3)(ClO_4)_2$. The CAMERON[20] projection with atomic labeling is shown in Figure 2c. The copper(II) ion is coordinated by three imidazole nitrogens and a thioether sulfur in the equatorial plane. The two ClO_4^- counterions are found in the apical positions at rather long distances from the copper(II) ion (2.90 and 2.96 Å). The geometry around the copper(II) ion is an elongated octahedron. Selected interatomic bond lengths and angles are given in Table 2.

Electrochemistry. Figure 3a shows the cyclic voltammogram of $Cu(L^1)(BF_4)_2$ in methanol. Two reduction steps are observed. The first redox step shows that the potential difference (ΔE_p) of the anodic and cathodic peaks is 0.14 V, and the second redox step shows $\Delta E_p = 0.21$ V; both follow a quasi-reversible process. The peak potentials are shown in Table 3. In order to investigate the nature of these peaks, experiments were carried out using various $L^1/Cu(BF_4)_2$ ratios, i.e. 1, 2, or 3 equiv of L^1 to 1 equiv of $Cu(BF_4)_2$. The cyclic voltammogram for 2 equiv of L^1 is redrawn in Figure 3b. Only one reduction process occurs at $E_{1/2} = 0.08$ V; this is also observed with 3 equiv of L^1 (data not shown). Two reduction steps are also observed for the Cu(II) complexes of the L^2 ligand with BF_4^- and Cl^- as counterions. The peaks and $E_{1/2}$ values are listed in Table 3.

In contrast, the cyclic voltammograms of the $Cu(L^3)^{2+}$ complexes show only one quasi-reversible process (see Figure 3c). The peak values and $E_{1/2}$ values are included in Table 3.

Electronic Studies. The UV–vis spectra of these Cu(II) complexes in methanol solution show a broad peak in the visible region ($(13.8–17.2) \times 10^{-3}$ cm^{-1}) due to the d–d transition (see Table 4). A higher energy peak (approximately 30×10^{-3} cm^{-1}) is also observed, which is assigned to the ligand to metal charge-transfer transition.[10] The λ_{max} and ϵ values are listed in Table 4. The vis–near-IR spectra of the solid state display various absorption peaks of which maxima are listed in Table 4.

EPR Studies. The EPR spectra of the polycrystalline powdered complexes recorded at room temperature are identical to those at liquid-N_2 temperature. However, the resolution of the low-temperature spectra is better; therefore, they were used to determine the EPR parameters.

The solid-state EPR spectrum of $Cu(L^1)(BF_4)_2$ recorded at 77 K is rhombic with $g_1 = 2.04$, $g_2 = 2.08$, and $g_3 = 2.13$. The complex $Cu(L^1)Cl_2$ shows an axial spectrum with $g_\parallel = 2.05$ and $g_\perp = 2.11$. The polycrystalline powder of $Cu(L^2)Cl_2$ also shows an axial spectrum with $g_\perp = 2.06$, but $g_\parallel$ could not be determined accurately. For $Cu(L^1)(BF_4)_2$, $Cu(L^1)Cl_2$, and $Cu(L^2)Cl_2$, no hyperfine coupling constant ($A_\parallel$) could be determined in the solid. It is usual in crystalline compounds where the copper ions are coordinated by not too large ligands, so that the copper ions are relatively close together, that the hyperfine splitting is not observed, due to paramagnetic exchange narrowing. The solid state EPR spectrum of $Cu(L^3)(BF_4)_2$ recorded at 77 K is axial with $g_\parallel = 2.21$, $g_\perp = 2.07$, and $A_\parallel = 177$ G.

In frozen solution (DMSO/CH_3OH; 1/1 v/v), only $Cu(L^3)(BF_4)_2$ presents an EPR signal that can be attributed to a single species (Figure 4a). In contrast, $Cu(L^1)(BF_4)_2$, $Cu(L^1)Cl_2$, and

Table 3. Cathodic (E_c) and Anodic (E_a) Potentials and $E_{1/2}$ Values (vs NHE) of Cu(II) Polyimidazole–Thioether Complexes in Solution

complex	E_c, V	E_a, V	$E_{1/2}$, V
$Cu(L^1)(BF_4)_2$	0.29	0.44	0.36
	–0.02	0.19	0.08
2:1 L^1:$Cu(BF_4)_2$	–0.02	0.19	0.08
3:1 L^1:$Cu(BF_4)_2$	–0.02	0.19	0.08
$Cu(L^2)(BF_4)_2$	0.19	0.39	0.29
	–0.08	0.16	0.04
$Cu(L^2)Cl_2$	0.24	0.46	0.35
	–0.07	0.10	0.02
$Cu(L^3)(BF_4)_2$	–0.01	0.12	0.06

Table 4. UV–Vis and Vis–Near-IR Data for the Cu(II) Polyimidazole–Thioether Complexes[a]

complex	UV–vis: λ_{max}, 10^3 cm^{-1} (ϵ, cm^{-1} M^{-1})	solid-state vis–near-IR, 10^3 cm^{-1}
$Cu(L^1)(BF_4)_2$	15.1 (90) (shoulder), 16.4 (100), 29.4 (2700)	12.7 (shoulder), 17.2
$Cu(L^1)Cl_2$	15.1 (120), 29.1 (4000), 37.3 (2750)	15.7, 22.3
$Cu(L^2)Cl_2$	15.1 (120), 29.4 (2500), 37.0 (2900)	15.7
$Cu(L^3)(BF_4)_2$	17.2 (65), 32.0 (2600)	17.2, 11.4 (shoulder)

[a] The UV–vis spectra were recorded in methanol solution at the concentration of 5×10^{-3}–5×10^{-4} M at 20 °C. The vis–near-IR spectra were recorded in the solid state.

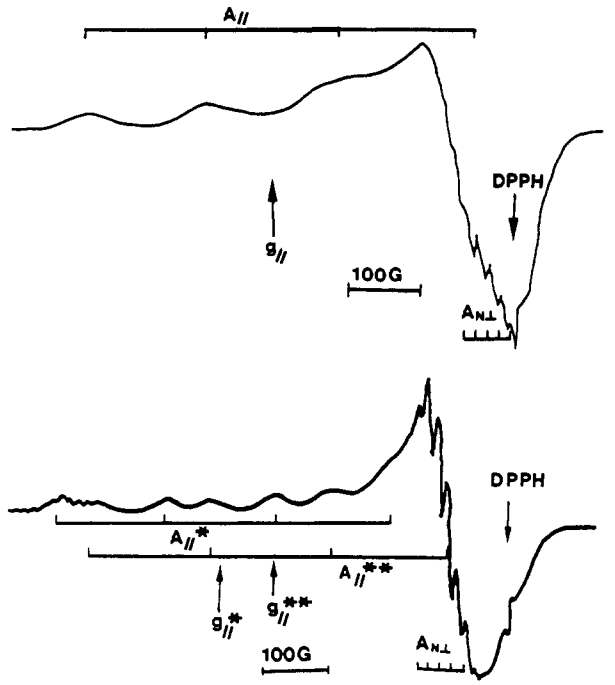

Figure 4. The X-band EPR spectra of (a, top) $Cu(L^3)(BF_4)_2$ and (b, bottom) $Cu(L^1)(BF_4)_2$ complexes in $DMSO/CH_3OH$ (1/1 v/v) solution obtained at 77 K. The symbols single and double asterisks represent the complex at different coordination spheres.

Table 5. EPR Parameters of the Cu(II) Complexes in Frozen-Solution CH_3OH/DMSO (1/1 v/v) at 77 K

complex	$g_\perp$	$g_\parallel$	$A_\parallel$, G	$A_{N\perp}$, G
$Cu(L^1)(BF_4)_2$	2.06	2.24	175	11.5
	2.06	2.30	170	12.8
$Cu(L^1)Cl_2$	2.06	2.22	179	11.5
	2.06	2.30	169	12.7
$Cu(L^2)Cl_2$	2.06	2.23	178	11.6
	2.06	2.30	171	12.8
$Cu(L^3)(BF_4)_2$	2.04	2.22	185	15.7

Table 6. NQI Frequencies (in MHz) Obtained from the ESEEM Spectra of Cu^{2+} Polyimidazole–Thioether Complexes in CH_3OH/H_2O

complexes	ν_0	ν_-	ν_+	η^a
$Cu(Him)_4^{2+}$ [b]	0.77	0.77	1.49	1.02
$Cu(bim)_2^{2+}$ [b]	0.64	0.96	1.61	0.75
$Cu(L^1)^{2+}$	0.60	1.03	1.65	0.67
$Cu(L^2)^{2+}$	0.64	0.96	1.60	0.75
$Cu(L^3)^{2+}$	0.64	0.93	1.64	0.75

[a] The asymmetry parameter η was estimated from the following equation: $\eta = 3\nu_0/(\nu_+ + \nu_-)$. [b] Reference 36.

$Cu(L^2)Cl_2$ present two overlapping EPR signals which may correspond to different coordination spheres (see Figure 4b). The $g_\perp$, $g_\parallel$, $A_\parallel$, and $A_{N\perp}$ parameters are listed in Table 5. The addition of excess ligands L^1 or L^2 to the appropriate solutions leads to the increase of one set of signals ($g_\parallel$ = 2.22–2.24; $A_\parallel$ = 174–179 G) over the other ($g_\parallel$ = 2.30; $A_\parallel$ = 168–170 G).

ESEEM Studies. Figure 5a shows the 3-pulse ESEEM spectrum obtained at 3400 G for a frozen solution of $Cu(L^2)^{2+}$ in CH_3OH/H_2O. This spectrum is similar to those obtained for Cu^{2+} complexes with imidazole type ligands.[21] Frequency peaks appear at 0.64, 0.96, 1.60, 2.23, 2.59, 3.21, and 4.56 MHz. The first three peaks at 0.64, 0.96, and 1.60 MHz are very close to those found for $Cu(Him)_4^{2+}$; they correspond to the three nuclear quadrupole interaction (NQI) transitions ν_0, ν_-, and ν_+ of the uncoordinated ^{14}N of the imidazole ligands (see ref 21). However, of particular note is the better separation of the first two peaks

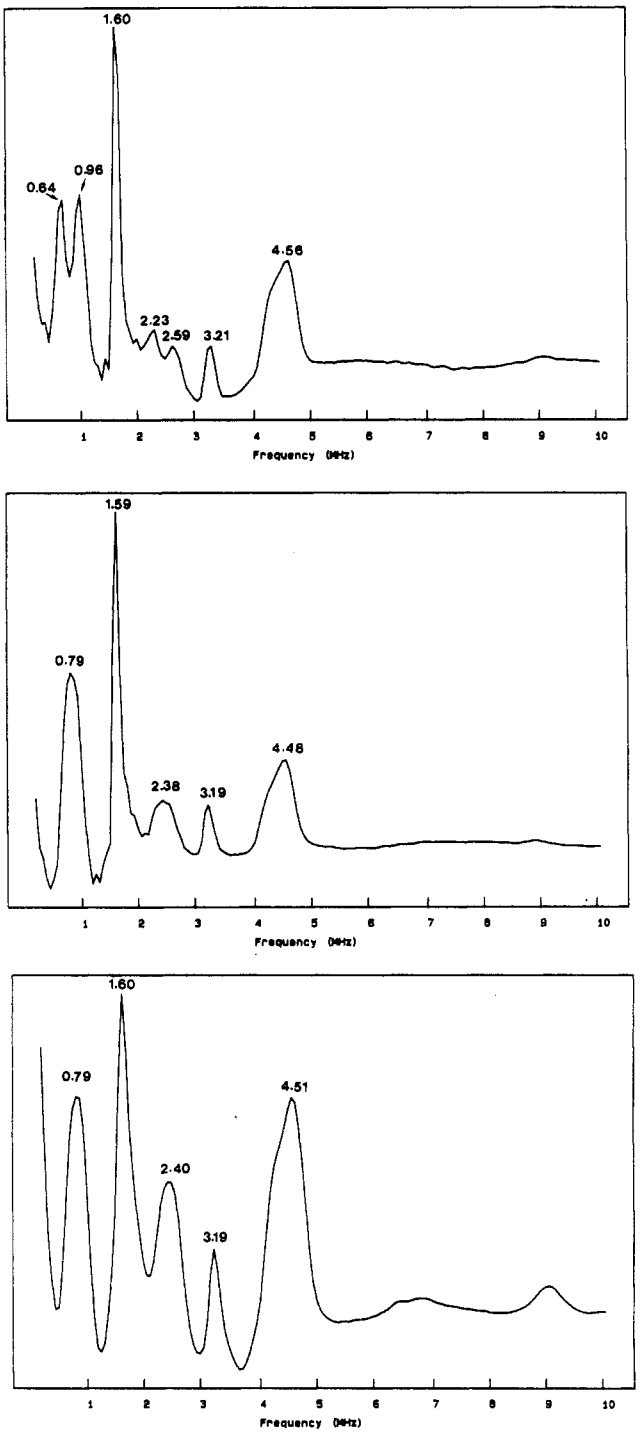

Figure 5. Three-pulse FT-ESEEM spectrum of (a, top) the mono-ligand $Cu(L^2)^{2+}$ complex dissolved in CH_3OH/H_2O, (b, middle) the mono-ligand $Cu(L^2)^{2+}$ complex dissolved in CH_3OH/DMSO, and (c, bottom) the bis-ligand $Cu(L^2)_2^{2+}$ complex dissolved in CH_3OH/DMSO. The data set was recorded at a temperature of 4.2 K, a magnetic field of H = 3400 G, a microwave frequency of 9.69 GHz, and a τ value of 136 ns. The interpulse time T was incremented from 88 to 6472 ns in 8-ns steps. Repetition time between successive pulse shots is 2.0 ms.

in Figure 5a, which overlap for $Cu(Him)_4^{2+}$ (see ref 21). This is indicative of a lower asymmetry parameter (η) of the NQI tensor of the uncoordinated ^{14}N (see Table 6). Jiang et al.[21] have shown that this reflects substitutions on the imidazole ring.

The spectra for the other two compounds, $Cu(L^1)^{2+}$ and $Cu(L^3)^{2+}$, obtained under the same conditions are very similar to that described here for $Cu(L^2)^{2+}$. Only very minor differences are observed in the peak positions. The results are summarized in Table 6.

The effect of the solvent on the ESEEM frequencies was also studied since its polarity may influence the electron spin density

(21) Jiang, F.; McCracken, J.; Peisach, J. *J. Am. Chem. Soc.* **1990**, *112*, 9035–9044.

at the uncoordinated N of the imidazole rings. Figure 5b shows the 3-pulse ESEEM spectrum obtained for $Cu(L^2)^{2+}$ dissolved in CH_3OH/DMSO. Comparison with Figure 5a shows that in DMSO, the first two peaks are no longer separated, indicating that the asymmetry parameter (η) is closer to 1 than in CH_3OH. Very similar effects were observed for $Cu(L^1)^{2+}$ and $Cu(L^3)^{2+}$ (data not shown).

When more than 1 equiv of ligand L^2 is used to complex 1 equiv of Cu^{2+}, one observes a significant increase in the amplitude of the lines at approximately 2.4 and 3.2 MHz in the spectrum, relative to those of the compound formed with 1 equiv of ligand (compare Figure 5b,c). Interestingtly, the same effect was observed for $Cu(L^1)^{2+}$ but not for $Cu(L^3)^{2+}$. The ESEEM spectra of the latter obtained with either one or two equivalents of ligand were virtually identical.

Discussion

In the Cu(II) polyimidazole–thioether complexes described here, the Cu–N bond distances are similar to those found in blue-copper proteins (2.04–2.10 Å in plastocyanin, 2.08 Å in azurin).[7,22,23] The Cu–N bond distances in $Cu(L^1)(BF_4)_2$ and in $Cu(L^2)Cl_2$ are in the range 1.94–2.06 Å, which is typically found for imidazole as an equatorial ligand in an axially elongated octahedral stereochemistry.[24] In the $Cu(L^3)(ClO_4)_2$ complex, one of the Cu–N distances is rather short (1.90 Å), even if one takes into account the poor precision of this distance. According to Dagdigian et al.,[24] the higher overall positive charge on a complex containing poorly coordinating anions is expected to result in shorter bond lengths compared to those of complexes with good coordinating anions, which fully compensate the charge on the copper. In the case of $Cu(L^3)(ClO_4)_2$, the oxygens of the ClO_4^- anions are at rather long distances to Cu (2.90 and 2.96 Å) due to a weak coordination of ClO_4^- with Cu, resulting in a higher overall charge on the complex and possibly leading to somewhat shorter Cu–N distance.

The Cu–S distances of 2.36 Å in $Cu(L^1)(BF_4)_2$, of 2.39 Å in $Cu(L^2)Cl_2$, and of 2.40 Å in $Cu(L^3)(ClO_4)_2$ all lie in the range of those reported for equatorial copper(II) thioether bonds (2.31–2.48 Å).[24,25] However, the Cu–S bond lengths of these complexes are much shorter than the Cu–S(methionine) distance (2.8–3.2 Å) found in the blue-copper proteins, where the thioether sulfur is in apical position.[7]

Much of the modeling work using polyimidazole N and thioether S ligands has been carried out using ligands where the thioether sulfur bridges two imidazole rings.[8] For example, the tridentate ligand 1,5-bis(4-imidazolyl)-3-thiapentane (bimtp)[26] coordinates with $CuCl_2$ to give crystals of $Cu(bimpt)Cl_2$ in an almost ideal trigonal-bipyramidal geometry. The two imidazole nitrogens are in the apical positions (Cu–N = 1.97 Å), and the thioether and the two chlorides form an equatorial plane with a Cu–S distance (2.50 Å) which is longer than that in the $Cu(L^2)Cl_2$ complex (2.39 Å). On the other hand, other studies[24,27] have described complexes coordinated in geometries that are similar to that of $Cu(L^2)Cl_2$. In these cases, the copper(II) coordinates with polyimidazole–thioether (N_2S) ligands in a square-pyramidal geometry; the fourth position of the equatorial plane and the apical position are occupied by solvent molecules or the anions.[24,27]

In literature many models consisting of tetradentate polyimidazole–thioether ligands, where two thioether sulfurs bridge two imidazoles, are described.[8] When the copper(II) is reported to be octahedrally coordinated, the two imidazole nitrogens are in the axial positions with Cu–N distances (1.93–1.97 Å) that are similar to those found in the present complexes, despite the fact that our imidazole nitrogens are in equatorial positions. On the other hand, in the literature, the two thioether sulfurs and the two counterions often form, an equatorial plane with rather long Cu–S distances (2.49–2.97 Å)[28-30] compared to those of our complexes (2.36–2.40 Å).

When the thioether sulfurs bridge the imidazole rings such as in the tridentate ligand bimtp discussed above, the thioether sulfur has a limited mobility in solution due to the rigidity of the ligand. Therefore, the S donor atom is kept or forced to stay in the coordination sphere of Cu(II). In contrast, in our new ligands, the thioether group is present at a terminal position and therefore it is more mobile. Furthermore, S is a soft ligand while Cu^{2+} is a relatively hard cation, contributing to the poor coordination of thioether sulfur with Cu^{2+} in solution. A likely equilibrium in solution is

$$2ML^{2+} \rightleftarrows ML_2^{2+} + M(\text{ligands})_n^{2+}$$

where ligands are possibly the solvent and a "free" imidazole of the macro ligand.

In the case of the L^3 ligand, the cyclic voltammetry shows only one set of quasi-reversible peaks. This indicates that the above equilibrium in this case is not observed, possibly due to the stability of the complex with three imidazole rings in the macro ligand, disfavoring the formation of the bis-ligand $M(L^3)_2^{2+}$ coordination sphere. On the other hand, the cyclic voltammograms of $Cu(L^1)^{2+}$ and $Cu(L^2)^{2+}$ solutions show two reduction peaks which are evidence for the presence of more than one type of coordination spheres in solution. For example, the voltammogram of $Cu(L^1)(BF_4)_2$ exhibits two sets of redox peaks at $E_{1/2}$ = 0.36 and 0.08 V. Using 2 equiv of ligand and 1 equiv of $Cu(BF_4)_2$, only the peak at 0.08 V is observed. This may show that the lower potential peak (0.08 V) corresponds to the bis-ligand complex $Cu(L)_2^{2+}$. This peak potential is indeed similar to that of the $Cu(L^3)(BF_4)_2$ complex (see Table 3), possibly reflecting the presence of about three imidazole nitrogens in the coordination sphere of this bis-ligand copper complex. It is noteworthy that the sharp oxidation peak of "free" $Cu(BF_4)_2$ in CH_3OH at 0.47 V (vs NHE) is not observed. Its absence might be due to the complex formation of the $M(\text{ligands})_n^{2+}$ with a part of the L^1 ligand which does not fully coordinate in the bis-ligand copper complex, and the potential of this complex could possibly be the higher potential peak (0.36 V), overlapping with the potential of the mono-ligand complex $Cu(L)^{2+}$.

As the number of S donor atoms increases, the Cu(II)/Cu(I) potential is expected to increase, possibly due to the stability of Cu(I) with S. The cyclic voltammetric study of the solution containing 1:1:1 bim:$Cu(BF_4)_2$:L^1 shows only one quasi-reversible peak at $E_{1/2}$ = 0.08 V, which is similar to the potential of the bis-ligand $Cu(L^1)_2(BF_4)_2$ (data not shown). The voltammogram of the $Cu(bim)_2(BF_4)_2$ solution exhibits only one quasireversible wave at $E_{1/2}$ = –0.02 V (data not shown). All three complexes, $Cu(L^1)_2(BF_4)_2$, $Cu(bim)(L^1)(BF_4)_2$, and $Cu(bim)_2(BF_4)_2$ have a set of four N donor atoms. However, the $E_{1/2}$ value of the two former complexes (0.08 V) is greater than that of the latter (–0.02 V), suggesting that the sulfur donor atoms are present in the coordination spheres of the bis-ligand $Cu(L^1)_2(BF_4)_2$ and the $Cu(bim)(L^1)(BF_4)_2$.

(22) Baker, E. N. *J. Mol. Biol.* **1988**, *203*, 1071–1095.
(23) Shepard, W. E. B.; Anderson, B. F.; Lewandoski, D. A.; Norris, G. E.; Baker, E. N. *J. Am. Chem. Soc.* **1990**, *112*, 7817–7819.
(24) Dagdigian, F. V.; McKee, V.; Reed, C. A. *Inorg. Chem.* **1982**, *21*, 32–1342.
(25) van Steenbergen, A. C.; Bouwman, E.; de Graaff, R. A. G.; Driessen, W. L.; Reedijk, J.; Zanello, P. *J. Chem. Soc., Dalton Trans.* **1990**, 3175–3182.
(26) Zoeteman, M.; Bouwman, E.; de Graaff, R. A. G.; Driessen, W. L.; Reedijk, J.; Zanello, P. *Inorg. Chem.* **1990**, *29*, 3487–3489.
(27) Addison, A. W.; Burke, P. J.; Henrick, K.; Rao, T. N. *Inorg. Chem.* **1983**, *22*, 1225–1228.
(28) Bouwman, E.; Burik, A.; ten Hove, J. C.; Driessen, W. L.; Reedijk, J. *Inorg. Chim. Acta* **1988**, *150*, 125–130.
(29) Bouwman, E.; ten Hove, J. C.; Driessen, W. L.; Reedijk, J. *Polyhedron* **1988**, *7*, 2591–2595.
(30) Bouwman, E.; Day, R.; Driessen, W. L.; Krebs, B.; Tremel, W.; Wood, J. S.; Reedijk, J. *Inorg. Chem.* **1988**, *27*, 4614–4618.

Nikles et al.[31] reported that the substitution of two amine donors by two thoether donors produced an increase in $E^{\circ\prime}$ of 0.3–0.7 V in pairs of the $(py)_2N_2$ and $(py)_2S_2$ complexes. Our results agree well with the empirical calculation of Bernardo et al.,[32] where the substitution of an S donor in L^1 with a N donor to form L^3 results in a decrease of 0.30 V in the Cu(II)/Cu(I) redox potential and where a further substitution of S by N to form the tim ligand ($E_{1/2}$ = –0.23 V) (data not shown) causes a decrease of 0.59 V in the Cu(II)/Cu(I) redox potential of L^1 complex. The increase in the number of N donor atoms causes a much more significant change in the redox potential of Cu(II)/Cu(I) compared to the increase in the number of S donor atoms. It is seen in Table 3 that the increase in number of S donor atoms from one S in L^2 ($E_{1/2}$ = 0.29 V) to two S in L^1 ($E_{1/2}$ = 0.36 V) results in a small increase of 0.07 V in the redox potential. This suggests that the dependence of the Cu(II)/Cu(I) potential on the relative number of N and S donor atoms is almost entirely a function of the preference of Cu(II) for N donor rather than the stability of Cu(I) toward thioether.[32]

The equilibrium between the mono- and the bis-ligand coordination spheres in solution is also observed in the electronic spectroscopic results and in the EPR and ESEEM studies. Only the $Cu(L^3)^{2+}$ complex shows the same peak at 17 200 cm^{-1} in the UV–vis (solution) and vis–near-IR (solid state) spectra (see Table 4). For the L^1 and L^2 Cu(II) complexes, the corresponding spectra give no common absorption peaks, showing that the d–d transitions are different in solution and in the solid state. For the two latter complexes, this suggests different coordination spheres of the complexes in solution and in the solid state. In the UV–vis study, the absorption coefficient ϵ (approximately 100 cm^{-1} M^{-1}) of the d–d transition in our complexes is similar to that of the d–d transition in normal copper coordination compounds.[33] The lack of the high ϵ value characteristic of the blue-copper proteins must be due to the absence of a thiolate group in our ligands.[10]

The EPR results show a good agreement with the electrochemical results on the formation of at least two types of Cu(II) coordination spheres in solution in the cases of L^1 and L^2 ligands. For the $Cu(L^1)^{2+}$ and $Cu(L^2)^{2+}$ complexes in solution, the $g_\parallel$ and $A_\parallel$ values are indicative of the presence of both the mono-ligand complex ($g_\parallel{}^*$ = 2.30; $A_\parallel{}^*$ = 168–170 G) and the bis-ligand complex ($g_\parallel{}^{**}$ = 2.22–2.24; $A_\parallel{}^{**}$ = 174–179 G) (Table 5). The Cu^{2+} complexes with solvents such as $Cu(CH_3OH)_n^{2+}$ or $Cu(DMSO)_n^{2+}$ could also be present in solution. However, their signals are probably too weak to interfere with the other signals. The addition of excess ligand leads to an increase in the EPR signal of the bis-ligand complex reflecting its increasing proportion at equilibrium. In the $Cu(L^3)(BF_4)_2$ complex, only one set of signals is observed ($g_\parallel$ = 2.22, $A_\parallel$ = 185 G). In all cases, the values of $A_\parallel$ are much larger than those reported for the blue-copper proteins.[2] This is again probably due to the absence of the thiolate group and of the typical distorted tetrahedral geometry around the Cu site that are found in blue-copper proteins.[34]

Decrease in the asymmetry parameter (η) of the NQI tensors of the uncoordinated nitrogen in the L^1, L^2, and L^3 complexes compared to $Cu(Him)_4^{2+}$ can be attributed to the effect of the substituents on the imidazole 2-position.[21] As noted above, the spectra of the three compounds are very similar to each other and also very similar to that of $Cu(bim)_2^{2+}$ (Table 6). In the $Cu(bim)_2^{2+}$ complex, the electron-donating effect of the Him–CH_2– group at the 2-position of the imidazole rings leads to a decrease in the polarity of the N–H bond and consequently a decrease of the electron occupancy of this bond. Jiang et al.[21] have shown that the electron occupancy of the N–H bond will influence the asymmetry parameter η of the uncoordinated nitrogen NQI tensor. For the three compounds studied here $Cu(L^1)^{2+}$, $Cu(L^2)^{2+}$, and $Cu(L^3)^{2+}$, the polarity of the N–H bond is decreased compared to that in $Cu(Him)_4^{2+}$ and this leads to a decrease in the asymmetry parameter from $\eta \approx 1$ for $Cu(Him)_4^{2+}$ to $\eta \approx 0.7$ (see Table 6). The L^1, L^2, and L^3 ligands also have the imidazole C4 position substituted with an electron-donating group; this does not seem to influence the ESEEM frequencies. This result is in agreement with the study of Jiang et al.[21]

The ESEEM peaks at approximately 2.4 and 3.2 MHz (Figure 5) correspond to combination frequencies of the fundamental NQI frequencies in Cu^{2+} compounds which contain more than one imidazole ligand, and the amplitude of the peaks can be related to the number of uncoordinated nitrogens.[35] In the presence of excess ligand, we expect the formation of the bis-ligand complexes for the L^1 and L^2 ligands but not for L^3. The increase in the amplitudes of the combination ESEEM peaks observed in Figure 5c compared to Figure 5b is consistent with the formation of the bis-ligand complex for L^2.

The asymmetry parameter of the NQI tensor of the uncoordinated N is higher for the $Cu(L_2)^{2+}$ complex in DMSO ($\eta \approx 1$) than for the same complex in H_2O ($\eta \approx 0.7$). This is explained as follows: DMSO has a stronger electric dipole moment (μ = 3.96 D) than H_2O (μ = 1.85 D). Therefore, the DMSO molecule forms stronger hydrogen bonds than does H_2O with the N–H of the remote nitrogen and this leads to an increase in the polarity of this N–H bond. This in turn leads to the increase in the electron occupancy of this bond. Very similar solvent effects have been reported by Jiang et al. in a recent ESEEM study of d_{z^2} ground-state Cu(II) complexes.[37]

Concluding Remarks

The present work models a part of the active site of the blue-copper proteins as two imidazole nitrogen donors and one thioether sulfur donor. However, in all complexes presented here, the thioether donor is in the equatorial position while it is in the apical position in the blue-copper proteins. As expected, the presence of the thiolate ligand is necessary to mimic the active site of blue-copper proteins. Due to the position of the thioether group in the macro ligand, an equilibrium of the mono- and bis-ligand complexes is established in solution, and this is confirmed by the various results described above.

Acknowledgment. K.C.T. is indebted to the Centre National de la Recherche Scientifiques for a postdoc position. We thank Dr. Willem Driessen for his constructive discussion and his useful comments and Dr. Hervé Bottin for the useful discussion on the structure of plastocyanin.

Supplementary Material Available: Tables of fractional atomic coordinates and U values of non-hydrogen atoms and of hydrogen atoms, anisotropic thermal parameters, interatomic bond lengths and angles, and experimental data for the crystallographic analysis and a figure showing a stereoview of $Cu(L^2)Cl_2$ molecules in the crystal lattice are available (10 pages). Ordering information is given on any current masthead page.

(31) Nikles, D. E.; Powers, M. J.; Urbach, F. L. *Inorg. Chem.* **1983**, *22*, 3210–3217.
(32) Bernardo, M. M.; Heeg, M. J.; Schroeder, R. R.; Ochrymowycz, L. A.; Rorabacher, D. B. *Inorg. Chem.* **1992**, *31*, 191–198.
(33) Solomon, E. I.; Lowery, M. D. *Science* **1993**, *259*, 1575–1581.
(34) Solomon, E. I.; Baldwin, M. J.; Lowery, M. D. *Chem. Rev.* **1992**, *92*, 521–542.
(35) McCracken, J.; Pember, S.; Benkovic, S. J.; Villafranca, J. J.; Miller, R. J.; Peisach, J. *J. Am. Chem. Soc.* **1988**, *110*, 1069–1074.
(36) Place, C.; Zimmermann, J. L.; Mulliez, E.; Chottard, J. C. Personal Communication. Data to be published.
(37) Jiang, F.; Karlin, K. D.; Peisach, J. *Inorg. Chem.* **1993**, *32*, 2576–2582.